Proceedings of IMECE2008
2008 ASME International Mechanical Engineering Congress and Exposition
October 31-November 6, 2008, Boston, Massachusetts, USA

IMECE2008-68048

Self-assembly of Rod-like Particles into 2D Lattices

M. Janjua, S. Nudurupati, I. Fischer and P. Singh
New Jersey institute of Technology
Department of mechanical Engineering
Newark, New Jersey – 07102
USA

N. Aubry
Department of Mechanical Engineering
Carnegie Mellon University
Pittsburgh, PA 15213
USA

ABSTRACT

It was recently shown by us that spherical particles floating on a fluid-fluid interface can be self-assembled, and the lattice between them can be controlled, using an electric field. In this paper we show that the technique can also be used to self assemble rod-like particles on fluid-fluid interfaces. The method consists of sprinkling particles at a liquid interface and applying an electric field normal to the interface, thus resulting in a combination of hydrodynamic (capillary) and electrostatic forces acting on the particles. A rod floating on the fluid interface experiences both a lateral force and a torque normal to the interface due to capillarity, and in the presence of an electric field, it is also subjected to an electric force and torque. The electric force affects the rods' approach velocity and the torque aligns the rods parallel to each other. In the absence of an electric field, two rods that are initially more than one rod length away from each other come in contact so that they are either perpendicular or parallel to the line joining their centers, depending on their initial orientations. In the latter case, their ends are touching. Our experiments show that in an electric field of sufficiently large strength, only the latter arrangement is stable. Experiments also show that in this case the electric field causes the rods of the monolayer to align parallel to one another and that the lattice spacing of a self-assembled monolayer of rods increases.

1. Introduction

In recent years much effort has been directed to understand the behavior of particles trapped at fluid-fluid interfaces because of their importance in a wide range of applications, e.g., the self-assembly of particles at fluid-fluid interfaces resulting in novel nano structured materials, micro/nano manufacturing, the stabilization of emulsions, etc. [1-7].

A popular mean used to assemble particles is based on the phenomenon of capillarity. A common example of capillarity driven self-assembly is the clustering of cereal flakes floating on the surface of milk. The floating cereal particles experience attractive capillary forces due to the fact that when two such particles are close to each other, the deformed interface around them is not symmetric as the interface height between the particles is lowered due to the interfacial tension. This lowering of the interface between the particles gives rise to lateral forces that cause them to move toward one another and cluster [7-10].

This naturally occurring phenomenon, however, leads to the uncontrollable clustering of particles, as capillary forces are attractive and increase with decreasing distance between the particles. As a result it produces monolayers that display many defects, lack order (both short and long ranged) and whose distance between the particles cannot be controlled. In addition, such a phenomenon does not manifest itself on particles smaller than ~10 μm. These drawbacks seriously limit the range of applications one can target using this technique.

The technique described in refs. [11-13] overcomes all these shortcomings (see figure 1) by applying an external electric field normal to the interface. The electric field causes spherical particles trapped at the interface to experience an electrostatic force normal to the interface and since the particles become polarized they also repel each other due to the dipole-dipole interactions. The former is a new phenomenon in which the electrostatic force arises because of the jump in the dielectric properties across the interface, and not because the applied electric field is nonuniform. In fact, an isolated particle subjected to a uniform electric field and suspended in a single fluid does not experience any electrostatic force. We also recall here that an interesting property of this interfacial phenomenon is that the electrostatic force thus generated varies as a^2, where a is the particle radius, and not as a^3, which is the case of the

well-known dielectrophoretic force [14,15] acting on particles suspended in a bulk liquid and under the influence of a nonuniform electric field. It follows that the new interfacial electrostatic force is stronger on small particles than the classic dielectrophoretic force. In addition, the resulting self-assembly process into two-dimensional arrays is capable of controlling the lattice spacing statically or dynamically, forming virtually defect-free monolayers of monodispersed spherical particles, and manipulating a broad range of particle sizes and types including nano-particles and electrically neutral particles. Indeed, the electric field causes particles to experience electrostatic and capillary forces, the magnitudes of which can be adjusted to control the lattice spacing of the formed monolayer.

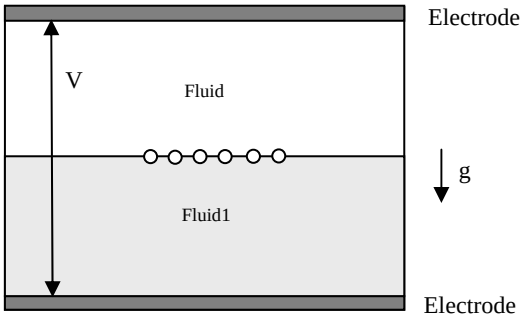

(a)

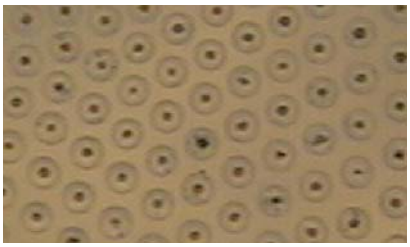

(b)

Figure 1. a. Schematic of the experimental setup used to control the self-assembly of particles on a fluid-fluid interface. The distance between neighboring particles is controlled by adjusting the applied voltage; b. Assembly of glass spherical particles obtained by using the device shown in (a) at an air-oil interface and with a voltage of 4000 V. The average radius of particles is 40.5 μm. Note the long range order, hexagonal and expanded lattice, which can be shrunk until the particles touch by decreasing the electric field strength.

In this paper, we apply the above technique to manipulate rods floating on an air-oil interface. In our experiments, rods float so that the cylinder axis is parallel to the interface and the contact line passes through both the cylindrical surface and the flat surfaces at the two ends. The problem of a rod floating on an interface is complex because in addition to the lateral capillary force, a rod also experiences a torque arising from the asymmetry of the interfacial deformation. Consequently, its interaction with other floating rods is more complex than that between spherical particles. Furthermore, the lateral capillary force is different along the normal and parallel directions to the rod's axis. As a result, there are certain stable arrangements in which two or more rods are likely to arrange, and which one of these arrangements is reached in a given case depends on their initial positions and orientations. In this paper we show that when an electric field is applied normal to the interface, rods become align approximately parallel to each other and the lattice spacing average of the monolayer increases with increasing electric field strength.

2. Electric and capillary forces on particles trapped at a fluid-fluid interface

The capillary and electric forces acting on a particle depend on the properties of the fluids and the particle, as well as on its position within the interface and the shape of the deformed interface. The equilibrium position of a particle in the interface can be obtained by solving the governing mass and momentum equations for the two fluids and the momentum equation for the particle, which are coupled, along with the interface stress condition and a condition for the contact line motion on the particle surface. The problem of finding the particle's equilibrium position itself is formidable because the vertical capillary force at the line of contact of the three phases on the particle surface depends on the slope of the interface which, in general, requires the solution of the governing equations and can be solved analytically only in simple situations [10,16].

The problem is even more challenging for a non-spherical particle, since the deformation of the interface and the capillary force depend on the direction of the normal to the particle's surface which depends on the location on the surface of the particle in a more complex manner than for a sphere [16,17]. The stability of a given orientation of a particle is also an important issue since a particle can float in one or more stable orientations which can be different for small and large sized particles of geometrically similar shapes. In addition, it is worth noting that the deformed interface around a non-spherical particle is non-symmetric and so the lateral capillary force due to such a particle depends on the radial direction from the particle's center which makes their clustering behavior more complex. In contrast, the deformed interface around an isolated spherical particle is symmetric about the vertical passing through its center, and thus the lateral capillary force that arises due to this deformation is independent of the radial direction from the sphere's center.

In general, for a non-spherical particle, the slope of the interface at the contact line is not constant, as the direction of the normal to the particle's surface varies. In fact, the slope of the tangent to the interface, which determines the vertical component of the capillary force acting on the particle, on a part of the contact line can be positive (the interface is deformed in the upward direction) while on the remaining part

it can be negative (the interface is deformed in the downward direction). As a result, although the total vertical capillary force is still equal to the buoyant weight, the contribution from some portions of the contact line to the vertical capillary force can be negative and from some other portions positive. The lateral capillary force and the torque normal to the interface between two or more particles are expected to depend on the shape of their deformed interfaces.

It is well known that two non-spherical particles can attract or repel depending on the interface deformation between them, i.e., if both particles cause upward or downward deformation of the interface, they attract; otherwise they repel. Depending on the form of the non-symmetric deformation around them, such particles can assemble into several different periodic arrangements, e.g., hexagonal or cubic. Also note that even a spherical particle can cause a non symmetric deformation of the interface if the contact line undulates on its surface [17]. These undulations in the contact line can arise because of the surface roughness caused by edges and irregular shape, chemical inhomogeneities, and Brownian motion. This can result in significant lateral capillary forces causing small particles with negligible buoyant weight to self assemble.

Although the focus of the present study is on rod-like particles, it is instructive to consider the behavior of spherical particles for which the closed form expression of the forces is available. The force balance in the vertical direction can be used to show that when the particle radius a approaches zero (small particles), the Bond number also goes to zero, i.e. $B=\rho_L a^2 g/\gamma \to 0$, where ρ_L refers to the density of the lower fluid, g denotes the acceleration due to gravity and γ stands for the interfacial tension. In this limit, the lateral capillary force which arises from the interfacial deformation is negligible compared to the random thermal forces, and so the latter force cannot cause particles to cluster. For particles floating on water, this limit is reached when the particles radius is approximately 10 μm (see [10,16]). Therefore, groups of small spherical and disk shaped particles cannot cluster by this mechanism. After reaching their respective equilibrium positions in the interface, such particles no longer substantially deform the interface. Small particles, however, can interact by means of other mechanisms [17]. Furthermore, when particles are partially immersed in a thin liquid film and their weight is supported by the substrate below, the arguments just given are not applicable and the interface deformation can be significant even for small particles [10].

It was shown in [11,12] that the above limitation for small particles can be overcome by applying an electric field normal to the interface. A particle floating at a fluid-fluid interface is subjected to an electric force normal to the interface which arises because of the mismatch between the dielectric constants of the two fluids involved, and thus the electric field around the particle is not symmetric about the fluid-fluid interface [11,12]. On the other hand, although an isolated uncharged particle placed in a uniform electric field inside a liquid becomes polarized, it does not experience any electrostatic force. As recalled in the introduction, it was shown that the dependence of the electrostatic force on the particle radius a is quadratic compared to the cubic dependence of the dielectrophoretic (DEP) force which acts on a particle in a non-uniform electric field [14,15]. The origin of the electric force acting on a particle at the interface is therefore different from that of the DEP force experienced by a particle immersed in a suspending liquid. In addition, the influence of electrowetting can be included by modifying the effective contact angle [28]. Notice that a change in the contact angle (due to electrowetting) will cause a particle to move normal to the interface in order to satisfy the new contact angle requirement. However, assuming that the only change is in the contact angle, it will not cause the interface to deform (because if the interface around the particle is deformed, the particle will experience a vertical capillary force which will remain unbalanced since the particle does not experience an additional external vertical force.). A rod floating on a fluid-fluid interface is also expected to experience an electric force normal to the interface. The dependence of this force on the rod's geometry is currently not known.

In the presence of an electric field, the lateral capillary force can be significant even when the Bond number approaches zero. This situation arises, for instance, for small particles when the magnitude of the electric field is sufficiently large. The equilibrium position of a particle within the interface in this case is determined by the balance of the interfacial and electrostatic forces. The interface can then be deformed by the particle, and the lateral (electric field induced) capillary forces are present and can cause nano sized particles within the interface to cluster [11, 12]. The electrostatic force thus plays a role similar to that of the particle's buoyant weight in causing lateral capillary forces. In addition, in the presence of an electric field (uncharged) particles become polarized and experience repulsive forces arising because of the dipole-dipole interactions [21,26].

The deformation of the interface due to trapped particles gives rise to lateral capillary forces which cause them to cluster (see figure 1) [8,10]. The attractive capillary forces arise due to the fact that when two floating particles are close to each other the interface height between the particles is lowered due to the interfacial tension. This lowering of the interface between the particles gives rise to lateral forces that cause them to come together. As noted above, the deformation of the interface is a result of the net vertical force acting on the particle, which includes its buoyant weight and the vertical electric force.

The electric field also results in the electrostatic repulsive force arising due to the dipole-dipole interactions which are short ranged (varying as r^{-4}). The attractive capillary forces, on the other hand, are long ranged (varying as r^{-1}). The dimensionless equilibrium separation, $r_{eq}/(2a)$, between two spherical particles, obtained by equating the repulsive electrostatic force and the lateral capillary force is

$$\frac{r_{eq}}{2a} = \frac{1}{2}\left(\frac{2\pi\varepsilon_0\varepsilon_a\left(\frac{\varepsilon_L}{\varepsilon_a}+1\right)\gamma E^2 f_D}{a\left(-\varepsilon_0\varepsilon_a\left(\frac{\varepsilon_L}{\varepsilon_a}-1\right)E^2 f_v + \frac{4}{3}\pi a\rho_p g\, f_b\right)^2} \right)^{\frac{1}{3}} . \quad (4)$$

The dimensionless parameters f_v, f_D and f_b depend on several parameters, and have to be obtained numerically or from experimental data. Here f_v, f_D and f_b are the dimensionless vertical force, electric repulsion and buoyancy force coefficients, and ε_p, ε_a and ε_L are the dielectric constants of the particle, the upper fluid and the lower fluid, E is the electric field strength and ρ_p is the particle density.

At present, an analysis similar to that presented above for spherical particles is not available for rod-like particles; particularly, the expressions for the electric and capillary forces and for the corresponding torques are not known. However, our experiments show that when rods floating on an interface are subjected to an electric field they experience dipole-dipole repulsive force, as well as an electric torque.

3. Results

We next present experimental results for the clustering behavior of borosilicate glass rods floating on the surface of corn oil. Experiments were conducted in a device for which the distance between the electrodes is 8 mm and the cross-section is circular with the diameter of 48 mm (see figure 1).

We first present results for two rods floating on the surface of corn oil. The rods were made by cutting borosilicate fibers. The diameter of the rods is 39.8 m, and the length of one rod is 255.2 m and of the second 260 m. The dielectric constant of corn oil is 2.87, its conductivity is 32.0 pSm-1 and its density is 0.922 g/cm3. The density of the borosilicate glass rods is 2.5 g/cm3 and their dielectric constant is 5.8. A variable frequency AC signal generator (BK Precision Model 4010A) was used along a high voltage amplifier (Trek Model 5/80) to apply a voltage to the electrodes at a frequency of 1 kHz. The applied voltage was 5000 V P/P (peak-to-peak). The motion of the rods was recorded using a digital color camera connected to a Nikon Metallurgical MEC600 microscope.

As already noted, in our experiments, rods float such that their axes are parallel to the interface. In this configuration, the interfacial deformation at the contact line on the curved surfaces is different from that at the flat ends. Thus, as discussed below, the lateral attraction due to capillarity is not the same along all radial directions. Notice that although the contact-angle condition is satisfied at both the curved and flat surfaces, the direction of the normal at the two surfaces is different, and as a result, the interfacial deformation at these surfaces is different. Experiments show that the attractive force in the direction perpendicular to the rod's axis is greater than in the parallel direction.

Three different initial configurations for the two rods were considered. In the first, the rods were parallel to one another and oriented perpendicular to the line joining their centers, in the second they were parallel to one another and parallel to the line joining their centers, and in the third they were perpendicular to each other. The initial distance between the rods was about 1.5 times their length. Next, we describe the behavior of the rods without and with the electric field. In the former case, the rods come together under the action of the force and torque due to capillarity, and in the latter case we show how this dynamics can be altered due to the additional presence of the electric force and torque.

3.1 Alignment in the absence of electric field

Experiments described below show that in the absence of electric field, the rods arrange themselves into one of the two stable configurations. In the first stable configuration, the rods are parallel to each other with their long sides touching, and in the second they are parallel to each other with their ends touching. The initial configuration of the rods determines which one of these stable configurations they evolve to. In the presence of an electric field of sufficiently large strength only the latter configuration is stable.

t=0 t=10 min

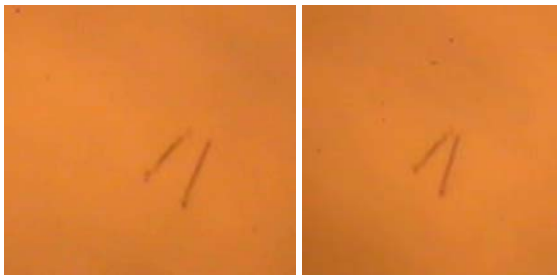

t=13min t=14 min

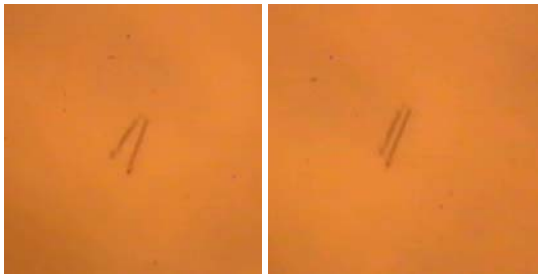

t=15 min t=21 min

Figure 2. Transient positions of two rods floating on the surface of corn oil. The electric field is turned off. The rods diameter is 39.8 μm and the length of the left rod is 255.2 μm and the right rod is 260 μm. Initially, the rods are approximately parallel. However, as they come closer to one another under the action of the lateral capillary force, they rotate so that their upper ends come in contact earlier. After coming in contact, the rods become approximately parallel again.

Figure 2 shows the case in which the two rods are initially approximately parallel to each other and the line joining their centers is perpendicular to the rods. The rods maintain this approximate orientation as they come closer. However, when the distance between them is approximately one half of their length, they rotate so that the upper ends of the rods come closer faster. This indicates that the attractive capillary force between the upper ends is larger than between the lower ends, and thus the rods are subjected to a net torque causing them to rotate so that the upper ends come closer faster. This becomes even more clear in the photograph taken at t=13 min. The rods continue to come closer and rotate with the rate of approach increasing as the distance between them decreases. The upper ends of the rods touch at t=14 min, and the lower ends touch at t=21 min. In this final configuration, the rods are again parallel to each other. It is noteworthy that the final orientation of the rods is arbitrary in the sense that it only depends on their initial orientations.

Furthermore, notice that the upper ends of the rods are closer than the lower ends which again is the result of the larger attractive force between these ends. For the case described above, the attractive capillary force between the upper ends is larger than between the lower ends because for the rods used in our experiments the geometry of the end planes varies, i.e., the angle between the normal to the rods' end planes and the rod's axis varies. In this case, the geometry is such that the attractive capillary force between the upper ends is larger than between the lower ends. Also note that the torque due to this asymmetry becomes significant only when the distance between the rods is about one-half of their length causing them to rotate, and that when the distance between the rods is larger they remain approximately parallel to each other.

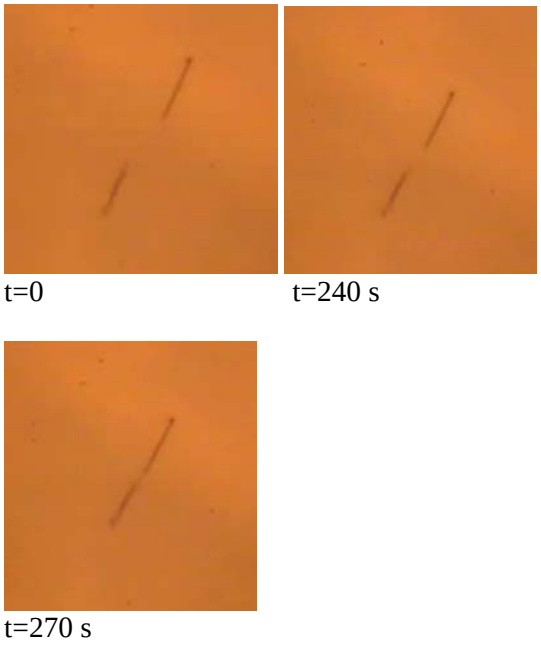

t=0 t=240 s

t=270 s

Figure 3. Attraction between two floating rods. The parameters are the same as in figure 2. The electric field is still turned off. Initially, the rods are approximately parallel to the line joining their centers. As they come closer, they align so that they are approximately parallel to the line joining their centers. In their final equilibrium position, the rods maintain this orientation and touch each other.

We next consider the case for which the two rods are initially approximately parallel to the line joining their centers (see figure 3). As before, the rods come closer under the action of the attractive capillary force while approximately maintaining their initial orientations. The approach velocity increases with decreasing distance between the rods. The approach velocity for this case is about three times smaller than for the case described in figures 2. This indicates that the lateral capillary force for this orientation of the rods is weaker. Notice that when the rods come in contact at t=270 s they are approximately parallel to the line joining their centers. This shows that this orientation of the rods is also stable and that if the rods are initially parallel to the line joining their centers they are likely to come together maintaining this orientation.

In figure 4 we present the case where initially the rods are approximately perpendicular to each other. They rotate under the action of the capillary torque (acting normal to the interface) to become parallel to each other, and afterwards their behavior is similar to that for the case described in figure 2 (not shown).

This shows that the preferred arrangement for the two rods (with a larger basin of attraction) is to align parallel to each other with their broad sides touching. Also, as noted above, the lateral capillary attraction between the rods for this

configuration is greater as the approach velocity is larger. However, if the rods are initially approximately parallel to the line joining their centers, they maintain this orientation while coming closer. After joining, they remain parallel with their ends touching.

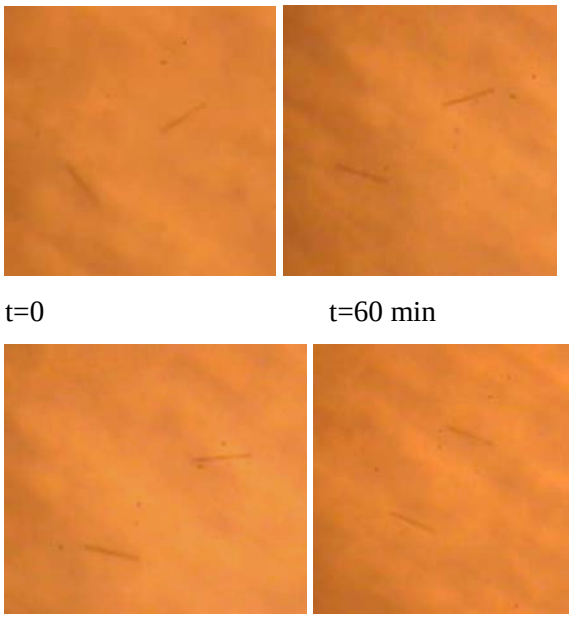

Figure 4. Attraction between two floating rods. The parameters are the same as in figure 2, except that initially the rods are approximately perpendicular to each other. The electric field is still turned off. The rods rotate to become approximately parallel to one another at t=270 min. Their motion after that point is similar to that in figure 2, and is thus not shown in this figure.

3.2 Alignment in presence of an electric field

We next consider the influence of an electric field normal to the interface on the motion and orientation of the rods as they come closer under the combined action of the electric and capillary forces. In figure 5 we consider the initial configuration which is similar to that in figure 3. The two rods are attracted to one another because of the attractive capillary forces, and their approach velocity increases with decreasing distance. As the rods come closer, they align along the line joining their centers. They touch at t=7 min 30 s. The approach velocity is approximately the same as for the case without electric field (see figure 6). This indicates that for this orientation of the rods the repulsive dipole-dipole force between the rods is relatively small, and does not significantly influence the rods' motion.

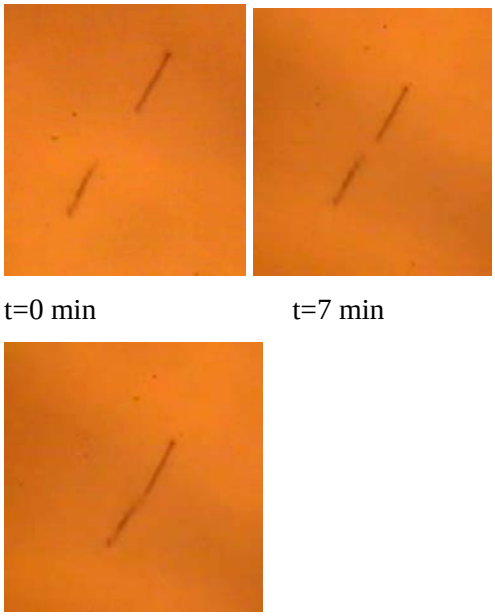

Figure 5. Attraction between two floating rods in the presence of the electric field. The device shown in figure 1 is subjected to a voltage of 5000 V. The other parameters are the same as in figure 3. As the rods come closer, they align along the line joining their centers. They maintain this orientation until touching.

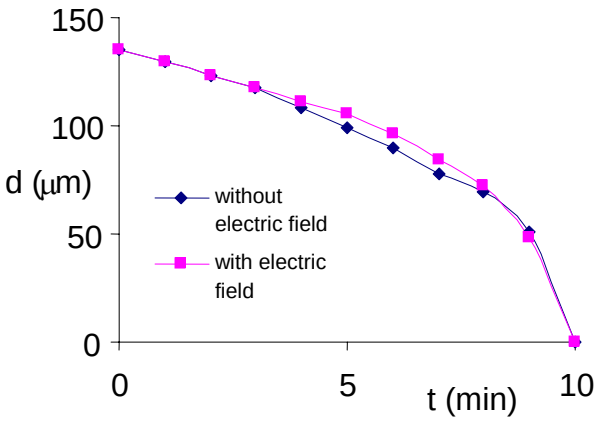

Figure 6. The distance between the rods' tips is plotted as a function of time for the experiments shown in figures 3 and 5 (with and without electric field). The rods are aligned parallel to the line joining their centers. Notice that the trajectories for the cases with and without the electric field are approximately the same. The voltage applied to the device is 5000 V.

t=0 min t=27min

t=28 min t=34 min

t=35 min t=35 min, 30 s

t=36 min

Figure 7. Attraction between two floating rods in presence of an electric field. The voltage applied is 5000 V. The other parameters are the same as in figure 2. Initially, the rods are approximately parallel, but when they are closer, they rotate so that the lower ends come in contact first. After coming in contact, the rods rotate so that the angle between them increases with time. In the final configuration, the rods align parallel to the line joining their centers with their ends touching.

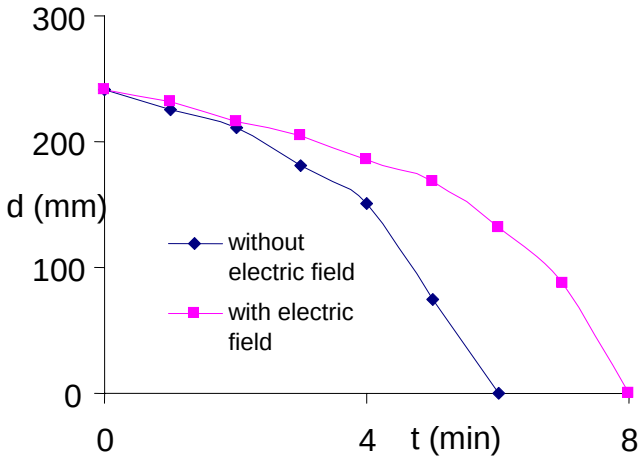

Figure 8. Distance between the rods' closest ends shown as a function of time in presence of an electric field, for the experiments shown in figures 2 and 7. Initially, the rods are oriented approximately perpendicular to the line joining their centers. Notice that the approach velocity is reduced in the presence of the electric field. The voltage applied is 5000 V.

t=0 t=150 min

t=360 min

Figure 9. Attraction between two floating rods in presence of an electric field. The voltage applied is 5000 V. The remaining parameters are the same as in figure 2. Initially, the rods are approximately perpendicular to each other. However, they rotate to become approximately parallel to the line joining their centers. The rods' behavior being the same as in figure 3 after t=360 min, the dynamics after that time is not reproduced here.

In figure 7 we consider the influence of the electric field on the attraction of two rods initially parallel and aligned approximately perpendicular to the line joining their centers. The rods come closer as time increases, with an average approach velocity about 1.4 times smaller than without the electric field, the latter case being described in figure 2. This decrease in the approach velocity is due to the repulsive dipole-dipole force between the rods. When the distance between the rods is greater than the rod length they remain approximately parallel, but when the distance is smaller than about one half of the rod length they rotate and the lower ends first come in contact. This was also the case in figure 2 without the electric field (although the upper ends came in contact first). Once the rods touch, they begin to rotate so that the angle between them increases. This is the opposite of what took place in figure 2, where the angle between the rods decreased. Here, in contrast the angle between the rods continues to increase until it becomes 180 degrees. The influence of the electric field is thus to align the rods so that in their equilibrium position they are parallel to the line joining their centers with their ends touching. We postulate that this rotation is due to an electric torque which arises because of the dipole-dipole interaction between the rods. From symmetry, the electric torque must be zero when the rods are parallel or perpendicular to each other.

We now seek to further verify that the influence of the electric field is indeed to align the rods along a common line. For this purpose, we consider the initial configuration in which the two rods are approximately perpendicular to each other (see figure 9). The rods rotate to become parallel to the line joining their centers, and afterwards their behavior is similar to that described in figure 7 (not shown in figure 9). We may therefore conclude that the preferred stable arrangement of two rods in the presence of electric field is to align parallel to the line joining their centers, with their ends touching. We remind the reader that the lateral capillary attraction between the rods makes them align perpendicular to the line joining their centers. This indicates that for the case shown in figure 9 the torque due to the electric field was sufficiently strong to overcome the torque due to capillarity.

We also considered the influence of the electric field on two rods that are initially in contact, with their long sides touching. The dipole-dipole repulsion causes the rods to move away from each other to a distance of about one rod diameter. The rods stop moving when this separation is reached. In some cases, two ends of the rods separate while the other two ends remain joined, thus resulting in the rods forming a “V” shape (see figure 10). The angle between the rods increases with increasing electric field strength and is larger for longer rods. After the electric field is turned off, the angle between the rods decreases and the rods return to their original equilibrium configuration. In some cases, the angle increases to 180 degrees and the rods become parallel. In these cases, even after the electric field is removed, the rods remain parallel to the line joining their centers with their ends touching.

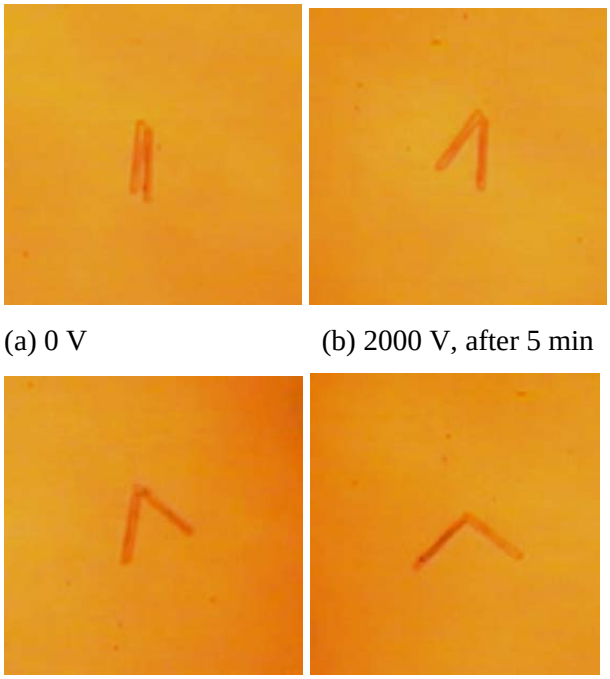

(a) 0 V (b) 2000 V, after 5 min

(c) 3000 V, after 15 min (d) 5000 V, after 30 min

Figure 10. Repulsion between two rods with their long side touching when a voltage is applied to the device. The rods assume a shape which looks like the letter “V”. The angle between the rods increases with increasing voltage.

4. Conclusions

Experiments show that two glass rods floating on the surface of corn oil cluster under the action of lateral capillary forces that arise because of the deformation of the interface. Since rods are also subjected to a torque due to capillarity, they come together either with their long sides touching or with their ends touching. In both cases they are parallel to each other.

In the presence of an electric field of sufficiently large magnitude, two rods released about one and half rod lengths away from each other arrange themselves to form a single line, i.e. they become parallel to the line joining their centers and come in contact so that their ends touch. This equilibrium arrangement is independent of their initial orientation. The electric field causes a rod on the interface to experience an electrostatic force normal to the interface. In addition, in an electric field the rods become polarized and interact with each other via dipole-dipole interactions. This results in a repulsive force and a torque. Furthermore, although the electric field causes rods to align parallel to each other, the direction of the alignment is not determined by the electric field which is normal to the interface. In experiments, the final direction of alignment depends on the rods’ initial orientations.

5. References

1. Aubry, N., P. Singh, M. Janjua and S. Nudurupati, Assembly of defect-free particle monolayers with dynamically adjustable lattice spacing, *Proceedings of the National Academy of Sciences*, 105, 10.1073/pnas.0712392105 (2008).

2. Aubry, N. and P. Singh, Physics underlying the controlled self-assembly of micro and nanoparticles at a two-fluid interface using an electric field, submitted to *Physical Rev. E* (2007).

3. Aubry N, Singh P (2007) Electrostatic forces on particles floating within the interface between two immiscible fluids, Paper IMECE2007-44095, Proceedings of 2007 ASME International Mechanical Engineering Congress and Exhibition, Nov. 11-15 Seattle, WA.

4. Murray CB, Kagan CR, Bawendi MG (2000) Synthesis and characterization of monodisperse nanocrystals and close-packed nanocrystal assemblies. *Annu. Rev. Mater. Sci.* 30: 545-610.

5. Tan Z, Zhang, Wang Y, Glotzer SC, Kotov NA (2006) Self-Assembly of CdTe Nanocrystals into Free-Floating Sheets, *Science* 314: 274-278.

6. Bowden N, Choi IS, Grzybowski BA, Whitesides GM (1999) Mesoscale self-assembly of hexagonal plates using lateral capillary forces: synthesis using the “capillary bond”, *J. Am. Chem. Soc.* 121: 5373-5391.

7. Bowden NA, Terfort A, Carbeck J, Whitesides GM (1997) Self-assembly of mesoscale objects into ordered two-dimensional arrays, *Science* 276: 233-235.

8. Grzybowski BA, Bowden N, Arias F, Yang H, Whitesides GM (2001) Modeling of menisci and capillary forces from the millimeter to the micrometer size range, *J. Phys. Chem. B* 105: 404-412

9. Wasielewski MR (1992) Photoinduced electron transfer in supramolecular systems for artificial photosynthesis, *Chem. Rev*. 92: 435.

10. Balzani V, Venturi M, Credi A (2003) Molecular devices and Machines, Wiley VCH, Weinheim.

11. Chan DYC, Henry JD, Jr. White LR (1981) The interaction of colloidal particles collected at the fluid interface, *J. Colloid Interface Sci*. 79: 410.

12. Fortes MA (1982) Attraction and repulsion of floating particles, *Can. J. Chem.* 60: 2889.

13. Kralchevsky PA, Nagayama K (2000) Capillary interactions between particles bound to interfaces, liquid films and biomembranes, *Advances in Colloid and Interface Science* 85: 145-192.

14. Lucassen J (1992) Capillary forces between solid particles in fluid interfaces. *Colloids Surf.* 65: 131-137.

15. Nicolson MM (1949) The interaction between floating particles, *Proc. Cambridge Philosophical Soc.*45: 288.

16. Singh P and Joseph DD (2005) Fluid dynamics of Floating particles, *J. Fluid Mech.* 530: 31-80.

17. Pohl HA (1978) Dielectrophoresis, Cambridge: Cambridge University Press.

18. Jones TB (1995) Electromechanics of particles, Cambridge University Press.

19. Stamou D, Duschl C (2000) Long-range attraction between colloidal spheres at the air-water interface: The consequence of an irregular meniscus. *Physical Rev. E* 62: 5263-5272.

20. Klingenberg DJ, Van Swol S, Zukoski CF (1989) Simulation of electrorheological suspensions, *J. Chem. Phys.* 91: 7888-7895.

21. Kadaksham J, Singh P, Aubry N (2004), Dynamics of pressure driven flows of electrorheological suspensions subjected to spatially non-uniform electric fields, *J. Fluids Eng.* 126: 170-179.

22. Kadaksham J, Singh P and Aubry N (2004) Dielectrophoresis of nano particles, *Electrophoresis* 25: 3625-3632.

23. Kadaksham J, Singh P and Aubry N (2005) Dielectrophoresis induced clustering regimes of viable yeast cells, *Electrophoresis*, 26, 3738–3744.

24. Kadaksham J, Singh P, Aubry N (2006) Manipulation of Particles Using Dielectrophoresis, *Mechanics Research Communications* 33: 108-122.

25. Aubry N, Singh P (2006) Control of Electrostatic Particle-Particle Interactions in Dielectrophoresis, *Euro Phys. Lett.* 74: 623–629.

26. Mugele F, Baret J (2005) Electrowetting: from basics to applications, *J. Phys.: Condens. Matter* 17: R705–R774.